Published in final edited form as:
Bone. 2008 November ; 43(5): 931–940. doi:10.1016/j.bone.2008.06.019.

Dual Delivery of an Angiogenic and an Osteogenic Growth Factor for Bone Regeneration in a Critical Size Defect Model

Zarana S. Patel[a], **Simon Young**[a], **Yasuhiko Tabata**[b], **John A. Jansen**[c], **Mark E.K. Wong**[d], and **Antonios G. Mikos**[a,*]

[a] Department of Bioengineering, Rice University, P.O. Box 1892, MS-142, Houston, TX 77251-1892 [b] Department of Biomaterials, Field of Tissue Engineering, Institute for Frontier Medical Sciences, Kyoto University, 53 Kawara-cho Shogoin, Sakyo-ku, Kyoto 606-8507, Japan [c] Department of Periodontology and Biomaterials, Radboud University Nijmegen Medical Center, THK17, P.O. Box 9101, HB6500, Nijmegen, The Netherlands [d] Department of Oral and Maxillofacial Surgery, University of Texas Health Science Center at Houston, 6516 M.D. Anderson Blvd., Suite DBB 2.059, Houston, TX 77030

Abstract

This study investigated the effects of dual delivery of vascular endothelial growth factor (VEGF) and bone morphogenetic protein-2 (BMP-2) for bone regeneration in a rat cranial critical size defect. Four groups of scaffolds were generated with VEGF (12 μg), BMP-2 (2 μg), both VEGF (12 μg) and BMP-2 (2 μg), or no growth factor released from gelatin microparticles incorporated within the scaffold pores. These scaffolds were implanted within an 8 mm rat cranial critical size defect (n = 8–9 for each group). At 4 and 12 weeks, implants were retrieved and evaluated by microcomputed tomography (microCT) and histological scoring analysis. Additionally, 4 week animals were perfused with a radiopaque material to visualize and quantify blood vessel formation. Histological analysis revealed that for all groups at 4 weeks, a majority of the porous scaffold volume was filled with vascularized fibrous tissue; however, bone formation appeared most abundant in the dual release group at this time. At 12 weeks, both dual release and BMP-2 groups showed large amounts of bone formation within the scaffold pores and along the outer surfaces of the scaffold; osteoid secretion and mineralization were apparent, and new bone was often in close or direct contact with the scaffold interface. MicroCT results showed no significant difference among groups for blood vessel formation at 4 weeks (<4% blood vessel volume); however, the dual release group showed significantly higher bone formation (16.1±9.2% bone volume) than other groups at this time. At 12 weeks, dual release and BMP-2 groups exhibited significantly higher bone formation (39.7 ± 14.1% and 37.4 ± 18.8% bone volume, respectively) than either the VEGF group or blank scaffolds (6.3 ± 4.8% and 7.8 ± 7.1% bone volume, respectively). This work indicates a synergistic effect of the dual delivery of VEGF and BMP-2 on bone formation at 4 weeks and suggests an interplay between these growth factors for early bone regeneration. For the doses investigated, the results show that the addition of VEGF does not affect the amount of bone formation achieved by BMP-2 at 12 weeks; however, they also indicate that delivery of both growth factors may enhance bone bridging and union of the critical size defect compared to delivery of BMP-2 alone.

*Corresponding author: Dr. Antonios G. Mikos, Department of Bioengineering, Rice University, P.O. Box 1892, MS 142, Houston, TX 77251-1892, Tel: (713) 348-5355, Fax: (713) 348-4244, mikos@rice.edu.

Keywords

Controlled release; Gelatin microparticles; Vascular endothelial growth factor; Bone morphogenetic protein-2; Bone tissue engineering

Introduction

Of the more than 6.2 million fractures that occur each year, approximately 5–10% will result in impaired healing and nonunions [1]. If there is no treatment undertaken in these cases, the patient will experience severe lifestyle impairment. Bone is a highly vascularized tissue and angiogenesis is crucial for bone regeneration [2]. Insufficient bone vascularity results in decreased bone formation and mass [3]. In addition, neovascularization helps support the mesenchymal stem cells and osteoblasts necessary for bone repair [2], and several studies have shown that osteogenesis is preceded by angiogenesis in a bone fracture model [4–8]. Thus, it is crucial to address the issue of angiogenesis in strategies for bone regeneration.

Controlled delivery of both angiogenic and osteogenic growth factors can mimic natural bone healing to promote the regeneration of critical size defects (CSDs) in animal models. CSDs are defects in which bone cannot regenerate sufficiently to bridge the length of the defect. Vascular endothelial growth factor (VEGF) is a potent angiogenic factor shown to be essential for both intramembranous [9] and endochondral bone formation [9,10] and in bone repair [11,12]. Bone morphogenetic protein-2 (BMP-2) is an osteogenic growth factor used extensively in both ectopic and orthotopic sites for bone generation [13]; it has been used for fracture sites and defects in rats [14], rabbits [15–17], and dogs [18]. Previous work by Kakudo et al. [19] delivered VEGF and BMP-2 from collagen hydrogels to an ectopic site (rat calf muscle) and demonstrated increased capillary density and bone formation at 3 weeks over sites which received BMP-2 alone. However, *in vivo* studies to evaluate the efficacy of delivering both VEGF and BMP-2 proteins in an orthotopic site to regenerate bone in a critical sized defect have not been performed.

In this study, we evaluated the angiogenic and osteogenic response to dual delivery of VEGF and BMP-2 for a rat calvarial CSD of 8 mm in diameter. Gelatin microparticles were utilized for the controlled release of the growth factors. These carriers have been used to provide controlled delivery of a variety of growth factors, including VEGF and BMP-2 as reported in previous *in vitro* and *in vivo* studies in our laboratory [20,21]. These studies demonstrated that crosslinking extents of the gelatin, as well as gelatin type, can be altered to provide tailored release profiles for each growth factor. For this work, acidic gelatin microparticles crosslinked with 10 mM glutaraldehyde were used for VEGF delivery [20], and basic gelatin microparticles crosslinked with 40 mM glutaraldehyde were used for controlled release of BMP-2 [21]. The microparticles were incorporated into a porous polymer scaffold made from poly(propylene fumarate) (PPF). PPF is biodegradable [22] and its biocompatibility in terms of soft and hard tissue response has also been demonstrated [23]. The porous PPF scaffold serves as a carrier for growth factor-loaded microparticles and can guide the development and growth of new tissue. In addition to typical histological evaluation of the implants, microcomputed tomography (microCT) techniques were utilized for quantitative evaluation of bone and blood vessel formation. This technique has proven to be a powerful analytical tool for assessing different bone regeneration therapies [24].

We hypothesized that the dual delivery of VEGF and BMP-2 would result in increased vascularity at 4 weeks and increased bony bridging and bone formation in the defects when compared with either growth factor alone at 12 weeks. To test this hypothesis, we implanted composite scaffolds into a rat cranial CSD and quantified blood vessel formation at 4 weeks,

and new bone formation at 4 and 12 weeks by microCT analysis. Histological analysis was also performed at both time periods.

Materials and Methods

Experimental Design

The experimental group ("DUAL") consisted of delivery of both VEGF (Peprotech, Rocky Hill, NJ) and BMP-2 (Peprotech, Rocky Hill, NJ) from gelatin microparticles confined within a porous PPF scaffold (composite scaffold). Controls consisted of single growth factor delivery ("VEGF" and "BMP-2" groups) and unloaded composite scaffolds ("BLANK"). An empty defect group was used for a negative control ("EMPTY"). In groups releasing a growth factor, 12 μg of VEGF (0.24 $\mu g/mm^3$) or 2 μg of BMP-2 (0.04 $\mu g/mm^3$) were delivered per implant. These doses were chosen based on previous *in vivo* work showing significant blood vessel formation or bone formation with those concentrations (amount per volume of implant) in a subcutaneous mouse model [25,26]. Based on previous work with rat cranial defects, the time periods chosen were at 4 weeks [27–30] and 12 weeks [31–33]. Four week animals were perfused with the contrast agent Microfil (Flowtech, Carver MA) after euthanasia to visualize the vasculature. At both time periods, microcomputed tomography (microCT) scans were conducted after harvest; in addition, the 4 week implants were decalcified and scanned again to quantify blood vessel formation alone. All groups consisted of $n = 8–9$ rats.

Gelatin Microparticle Preparation

5 g of gelatin (Nitta Gelatin Co., Osaka, Japan) were dissolved in 45 mL of water and added dropwise to 200 mL olive oil to create a water-in-oil emulsion [34]. The solution was stirred at 500 rpm and chilled to 10°C for 1.5 hours; microparticles were then collected by washing with acetone and vacuum filtration. They were crosslinked overnight in a glutaraldehyde solution and the reaction was terminated by the addition of glycine (25 mg/mL) to block residual aldehyde groups. The microparticles were again washed in acetone and collected by filtration, lyophilized, and then sieved to obtain particles ranging in diameter from 50–100 μm.

Acidic and basic gelatin microparticles were crosslinked with 10 mM and 40 mM glutaraldehyde and used for loading of VEGF and BMP-2, respectively. Growth factor incorporation was achieved by diffusional loading; a solution of growth factor in PBS was dripped onto the microparticles at a volume of 5 μL per mg of dry microparticles. Following vortexing, the loaded microparticles were incubated at 4°C for 20 hours.

PPF Synthesis

PPF synthesis involved the generation of a diester intermediate followed by polymerization [35]. First, diethyl fumarate, propylene glycol, hydroquinone, and zinc chloride were combined in a 1:3:0.003:0.01 molar ratio and stirred at 300 rpm and heated to 130°C under a nitrogen purge. Ethanol was distilled out and the reaction was stopped when 90% of the theoretical yield of ethanol was removed. The temperature was then set to 100°C and vacuum (<1 mmHg) was applied. Every 30 min, the temperature was raised 10°C to 130°C and maintained while propylene glycol was removed as a distillate. Samples were collected every hour for GPC analysis and the reaction was terminated once the desired molecular weight was reached. Purification was achieved through a 1.85% hydrochloric acid wash followed by a series of aqueous washes to remove zinc chloride and an ether wash to remove hydroquinone. The purified polymer was then vacuum dried to eliminate any residual solvent. The final number average molecular weight as determined by GPC was 1770 with a polydispersity index of 1.7.

Porous PPF Scaffold Fabrication

To generate porous polymer scaffolds, PPF and N-vinyl pyrrolidone were mixed together in a 1:1 mass ratio; this was followed by addition of 0.5 wt% benzoyl peroxide (0.1 mg/mL in acetone) and 80 wt% NaCl (300–500 μm crystals) [36]. This paste was packed into molds (8 mm diameter, 1 mm height) and crosslinked overnight at 60°C. The scaffolds were leached in water for 3 days to remove the salt, resulting in a porous structure. These porous PPF scaffolds were then lyophilized overnight, and the surface areas were sanded down to achieve a height of 1 mm. Following flushing with 70% ethanol, the scaffolds were again lyophilized overnight.

Composite Scaffold Generation

Composite scaffolds consisted of gelatin microparticles entrapped within the pores of the PPF scaffolds. 2.5 mg each of acidic and basic gelatin microparticles were mixed together in 30 μL of a 24% (w/v) solution of Pluronic F-127 (Sigma Aldrich, St. Louis, MO) in water, injected into a porous PPF scaffold, and allowed to gel at room temperature for 10 min [37]. Depending on the experimental group, the acidic 10 mM or basic 40 mM microparticles were either loaded with VEGF or BMP-2, respectively, or swollen with PBS alone. For control scaffolds, both types of microparticles were swollen with PBS only.

Animal Surgeries and Euthanasia

This work was conducted in accordance with the National Institutes of Health animal care and use guidelines. Microparticles, PPF scaffolds, and dry Pluronic were sterilized by ethylene oxide. Water and PBS were syringe-filtered with 0.22 μm filters. After the composite scaffolds were synthesized, they were implanted into a rat cranial defect. 12 week old male syngeneic Fischer-344 rats (Harlan, Indianapolis, IN) weighing approximately 175–225 grams were used for the surgeries. Each animal was anesthetized with a 4% isoflurane and oxygen mixture and then shaved around the incision area. An intraperitoneal injection of buprenorphine (0.05 mg/kg) for post-operative analgesia was given, and the animal was transferred onto a heating pad (maintained at 37°C) in the operating field. Anesthesia was maintained with a 2% isoflurane/oxygen gas mixture during surgery. A subcutaneous injection of 0.5 mL of 1% lidocaine as a local anesthetic was given along the sagittal midline of the skull. Following this, a sagittal incision was made over the scalp from the nasal bone to the middle sagittal crest and the periosteum was bluntly dissected. An 8 mm defect was created using a dental surgical drilling unit with a trephine constantly cooled with sterile saline; subsequently, the calvarial disk was carefully removed to avoid tearing of the dura. After thoroughly rinsing with physiological saline to wash out any bone fragments, a composite scaffold was implanted within the defect. The periosteum and scalp were closed over in layers with interrupted 4-0 Vicryl resorbable sutures. After surgery, the animal was given a subcutaneous injection of sterile saline (10 mL/kg/hr of surgery) and kept on pure oxygen until it awakened from anesthesia. The rats were placed into soft-bedded plastic cages and housed individually after the procedure. Each animal received a subcutaneous injection of buprenorphine (0.05 mg/kg) at 12, 24, and 36 hours after surgery for continued postoperative analgesia. Animals had free access to food and water and were monitored daily in the postoperative period for any complications or abnormal behavior. At 4 and 12 weeks after surgery, rats were euthanized for implant retrieval. After anesthesia with 4.5% isoflurane/oxygen, the gas was switched to carbon dioxide for asphyxiation followed by a bilateral thoracotomy as a secondary method of euthanasia.

Microfil Perfusion

All 4 week samples were perfused with Microfil (Flowtech, Carver, MA) after euthanasia to evaluate blood vessel formation. The chest was shaved and an incision was made from the

front limbs down to the xyphoid process. Scissors were used to cut along one side of the sternum and the rib cage was retracted laterally. The descending aorta was clamped and an angiocatheter was used to penetrate the left ventricle. The inferior vena cava was incised and immediately after, perfusion of 20 mL of heparanized saline was started (100 U/mL at 2 mL/min using a syringe pump). A solution of Microfil was prepared in a volume ratio of 4:5 of Microfil:diluent with 5% curing agent. Following perfusion with saline, 20 mL of the Microfil solution was perfused at 2 mL/min. Finally, the Microfil was allowed to set overnight at 4°C.

Implant Retrieval

To harvest the implants, an incision was made between the medial canthi of the eyes down to the bone. A 701 burr attached to a Stryker Total Performance System straight handpiece at 40,000 rpm was used to cut through the bone with water irrigation. Similar cuts were made along the left and right temporal bone and posterior aspect of the cranial vault. This resulted in a rectangular section of the cranium, including the defect site and implant, which was removed and placed into 10% neutral buffered formalin. For 4 week implants, the brain and skin tissue were kept in place to minimize tearing of blood vessels within the defect. At 12 weeks, the brain and skin were excised.

Microcomputed Tomography (microCT)

MicroCT analysis provided a means of quantitatively measuring the amount of bone and blood vessel formation within the defect. All samples were scanned after implant retrieval with a SkyScan 1172 high-resolution microCT imaging system (Aartselaar, Belgium) at a 10 μm resolution with 0.5 mm aluminum filter and a voltage of 100 kV and current of 100 μA. Volumetric reconstruction and analysis were conducted using Nrecon and CT-analyser software provided by SkyScan. A global threshold of 45–255 was used for these initial scans. The 4 week samples were scanned again after decalcification at a 12 μm resolution to quantify only blood vessel formation; a threshold of 30–255 was used for these scans. To calculate the percent of bone or blood vessel formation within the defect, a cylindrical volume of interest (VOI) of 8 mm in diameter and 1.5 mm in height was centered over the defect. The VOI for 4 week samples was placed above the sagittal sinus since variability in the size and presence of this sinus can affect the measurements of blood vessel formation. For 12 week samples, the VOI was placed at the bottom of the defect since the brain, and thus the sagittal sinus, were removed during harvest. Data are reported as the % binarized object volume measured within this VOI with the CT-analyser software.

The extent of bony bridging and union within the defect was scored according to the grading scale in Table 1. These scores were determined from maximum intensity projects generated from the microCT datasets in the CT-analyser software. Three-dimensional models of the samples were also constructed as needed in order to determine a score for union.

Histological Processing

The samples were fixed for 7 days in 10% neutral buffered formalin and then placed in 70% ethanol for the duration of the microCT scans. After scanning, the 4 week samples were decalcified in 5% formic acid at 37°C for 5 days with daily solution replacement. All samples were dehydrated in a graded series of ethanol (from 70% to 100%) and embedded in methylmethacrylate. Following polymerization, a modified diamond saw technique was used to make 10 μm coronal sections [38]. At least three sections were taken from each sample and stained with methylene blue/basic fuschin.

Light Microscopy and Histological Scoring

The three sections from each sample were evaluated via light microscopy and scored with a quantitative grading scale (Table 2). Samples were assessed for: (1) quality of the bone-scaffold interface; (2) tissue response within the pores of the scaffold; and (3) quantity of bone formation within the defect. Two blinded reviewers (ZSP and SY) separately evaluated 3 sections per sample and reached a consensus on the score for each section. The scores were averaged for each sample and then averaged for each group to determine the overall score for the group.

Statistics

Multi-factor analysis of variance was performed followed by a Tukey-Kramer multiple comparisons test using SAS statistical software (Cary, NC). Differences between groups were considered statistically significant at $p<0.05$ for $n = 8–9$.

Results

Descriptive light microscopy

Four different groups of scaffolds were implanted: those with both VEGF and BMP-2 (“DUAL”), those with either growth factor alone (“VEGF” and “BMP-2”), and scaffolds with no growth factor (“BLANK”). Gross examination of the sections was performed for all samples. For all conditions with a scaffold implant, the PPF scaffold and its porosity (due to the NaCl crystals as porogens) were clearly visible. At both 4 and 12 weeks, a thin fibrous capsule was observed around the periosteal side of the scaffolds, as well as at some interfaces at the defect border. At 4 weeks, a majority of the samples showed infiltration of immature fibrous tissue within the scaffold pores (Figure 1). Bone formation in the BLANK and VEGF groups was minimal, while the BMP-2 and DUAL groups showed visibly higher amounts of bone formation within the scaffold pores. Microfil perfusion allowed for easy identification of blood vessels within the sections due to the dark brown-black coloring of the Microfil (Figure 1B, black arrow). However, in some sections, incomplete perfusion of blood vessels of varying sizes was also observed (white arrows). Vessel diameter was variable but almost all vessels were less than 100 μm in diameter, and many averaged about 50 μm in diameter. Additionally, most blood vessels observed by histology did not show maturation as characterized by the presence of a media or the recruitment of pericytes; instead, only the endothelium was present.. Finally, some scaffold fragmentation was visible at 4 weeks and increased at 12 weeks, but the inflammatory response was minimal, with only a few inflammatory cells (neutrophils, macrophages) present.

At 12 weeks, many of the BMP-2 and DUAL groups showed a notable amount of bone formation compared to the other groups, both within the pores and along the outer surface of the scaffold (Figure 2). This guided bone formation was observed mostly on the dural side (Figure 2E) although there were also samples that showed similar formation along the periosteal side. Intramembranous ossification was apparent within the pores and characterized by osteoid secretion and mineralization (Figure 2F, white arrows). In these cases, the new bone was often in close or direct contact with the scaffold, without an intermediate fibrous layer present. The BLANK and VEGF groups showed only minimal bone formation within the scaffolds and pore tissue consisted mostly of dense, vascularized fibrous tissue. Additionally, empty defects were not healed at 12 weeks.

Quantitative histological analysis

Samples were evaluated for the quality of the bone-scaffold interface, tissue response within the pores, and bone formation within the defect (Figure 3). Figure 3A shows the scoring results for the hard tissue response at the bone-scaffold interface. There was no difference in

groups at 4 weeks but the 12 week groups showed increasing scores (better scaffold integration) from BLANK to DUAL groups. At 12 weeks, the DUAL group was significantly different from BLANK and VEGF groups ($p<0.05$).

The scoring of hard tissue response within the scaffold pores is shown in Figure 3B. At 4 weeks, the DUAL group had the highest score (2.4) with mostly immature fibrous tissue with and without bone, while the other groups all had similar, lower scores (<1.8). At 12 weeks though, only BMP-2 was significantly different from its 4 week counterpart.

Scoring of bone formation (Figure 3C) within the 4 week groups showed the DUAL group to have significantly more bone than BLANK or VEGF groups, but not BMP-2. As with pore tissue scores at 12 weeks, only BMP-2 showed a significant difference for bone formation from its 4 week group; it also had higher scores than the BLANK or VEGF groups at 12 weeks ($p<0.05$).

MicroCT analysis

Samples were evaluated for bone and blood vessel formation using microCT as a nondestructive method. Maximum intensity projections (generated from microCT software) of each group were used (Figure 4) for the scoring of bony bridging across the defect. Figure 5 shows the results of this scoring for 4 and 12 week groups. BMP-2 and DUAL groups showed significantly higher scores for union compared to VEGF groups at both 4 and 12 weeks; at 12 weeks, the DUAL group was also significantly higher than the BLANK group.

At 4 weeks, blood vessel formation was quantified by perfusing the animal vasculature with Microfil (a radiopaque agent) and scanning after decalcification. Bone volume was calculated from the difference in microCT scans of samples before and after decalcification. At 12 weeks, the samples were not perfused with Microfil and only bone volume was quantified. Data are reported as % binarized object volume within a given VOI. It should be noted that given the method of drawing the VOI, and that the scaffold was expected to have only minimal degradation, the % object volume within the VOI will never be 100%. Even if all the porous volume within the scaffold (approximately 70% based on previous studies) was filled with bone or blood vessels, the % object volume would be less than 70% given that the VOI is drawn to be 1.5 mm in height while the scaffold is synthesized to be 1 mm in height.

Figure 6 depicts % blood vessel volume within the VOI at 4 weeks. Although the VEGF group had the highest amount of blood vessel formation, there was no significant difference between any of the groups. The % bone volume within the VOI at 4 and 12 weeks is shown in Figure 7. As can be seen, bone formation in the DUAL group was significantly higher than all other groups at 4 weeks. At 12 weeks, both BMP-2 and DUAL groups showed significantly more bone formation than EMPTY, BLANK, and VEGF groups but not from each other. It should also be noted that % bone volume for the 4 week empty defect may be an underestimation in some cases. This is due to how the VOI was drawn for 4 weeks (resting above the sagittal sinus) and the observed protrusion of the sagittal sinus and brain into the defect area of empty groups.

Discussion

The objective of this study was to evaluate the efficacy of a dual growth factor release system for healing of an 8 mm critical size bone defect. We hypothesized that the dual delivery of an angiogenic factor with an osteogenic factor would result in a synergistic response to produce increased bony bridging and bone formation within the CSD compared with either growth factor alone. We theorized that the augmented osteogenic response would

be the result of a stimulated formation of a network of blood vessels by VEGF within the defect and this vascular system would recruit and support osteoprogenitor cells. Implants with dual growth factors, single, and no growth factor were placed within 8 mm critical size rat cranial defects. These implants were harvested at either 4 or 12 weeks and scanned via microCT and processed for histological analysis. The use of the radiopaque agent Microfil at 4 weeks allowed for visualization and quantification of the vasculature. This technique has been used in previous work for the evaluation of both bone formation [39] and blood vessel formation [40].

At 4 weeks, microCT data showed no significant differences of % blood vessel volume among groups. However, we have previously shown that VEGF released from the same delivery system used in this study is still bioactive at 2 weeks in a cell culture assay, and the response of endothelial cells is dose-dependent [20]. Additionally, earlier work using mineralized or glass-coated poly(lactide-*co*-glycolide) scaffolds for VEGF delivery has shown increased blood vessel formation over controls without VEGF at 2 weeks in a rat cranial CSD [41,42] using smaller amounts of growth factor (3 μg per animal). Therefore, it is possible that the effect of VEGF on angiogenesis played out at an earlier time and is not seen at the 4 week time period. Also, the presence of VEGF by itself cannot result in a mature blood vessel network, and if its concentrations fall below critical levels, the blood vessel network is unstable and can be remodeled or trimmed [43]. In this case, an earlier 2 week time point may show more significant differences between groups for blood vessel formation.

Consideration should also be given to the limitations of using contrast-enhanced microCT for the quantification of blood vessel networks. Although this technique has been successfully used to characterize neovascularization in a variety of animal models [40,44], scan resolution may be an issue if the detection of capillary-sized vessels is desired. In the present study, a nominal scan resolution of 12 μm was chosen for vessel quantification while still allowing for the appropriate field of view necessary to image the entire cranial bone defect. However, capillary-size vessels (smaller than 12 μm) were not quantified at this resolution. This limitation combined with the fact that VEGF likely had the most impact on capillary formation could also account for the lack of a significant difference in blood vessel volume among the groups at 4 weeks.

MicroCT analysis of bone formation at 4 weeks showed significantly higher % bone volume for the dual release of VEGF and BMP-2 than all other groups. This increased bone formation at 4 weeks is similar to results from Akita et al. [45] in which BMP-2 and bFGF were delivered with mesenchymal cells via a gelatin sponge carrier in a 4 mm rat cranial defect (not a critical size defect); higher bone mineral density was observed with the dual release group compared with only cells in the sponge or only phosphate buffered saline. However, they did not make comparisons with single growth factor delivery.

To interpret these results, one should consider the multiple effects that VEGF and BMP-2 can have on different cell types and what role each growth factor plays in angiogenesis and osteogenesis. VEGF is a potent angiogenic growth factor and causes proliferation and migration of endothelial cells. However, it has also been shown to promote chemotaxis [46] and differentiation of osteoblasts [11,47]. Similarly, BMP-2 can also possess pleiotropic functions: firstly, it is a potent osteogenic growth factor, driving osteoprogenitor cell differentiation and proliferation. It can also act as an indirect angiogenic factor, stimulating osteoblast production of VEGF [48] and serving as a chemoattractant for endothelial cells [49].

This property of VEGF to promote chemotaxis and differentiation in osteoblasts can result in a synergism with BMP-2 to result in the increased bone formation observed from the dual release group at 4 weeks. The observed bone formation may also be a result of a dose effect, since the dual release groups receive a total of 14 μg of growth factor, while VEGF groups receive 12 μg and BMP-2 groups receive 2 μg. However, if it was a simple dose effect, there would also be significantly higher % blood vessel volume for the dual release group at 4 weeks; this was not observed. It is possible that the dose of VEGF chosen for this study was not optimal for vessel formation within a healing bone defect, given that it was based on delivery within a subcutaneous site [25]. Previous studies involving the release of VEGF in rat cranial defects show that amounts of 3 μg per animal were effective in promoting neovascularization over controls [41,50,51]. While the main focus of this study did not involve the determination of growth factor dose effects, further investigations with varying doses can help clarify the mechanism of action.

Also of note, VEGF delivery alone at 12 μg per defect was found to have no impact on bone regeneration at both 4 and 12 weeks in this study. Interestingly, this finding contrasts previous work by Kaigler et al. which demonstrated increased bone regeneration over controls when VEGF-releasing PLGA scaffolds were implanted in a pre-irradiated, non-critical size rat cranial defect [50]. Groups releasing VEGF were found to have statistically significant increases in bone formation versus their unloaded PLGA scaffold controls in both irradiated and non-irradiated defects at 6 and 12 weeks. However, differences in the delivery vehicle (PPF scaffolds incorporating VEGF-loaded gelatin microparticles versus PLGA scaffolds incorporating VEGF directly), VEGF dose (12 μg versus 3 μg) and the animal model (8 mm critical size defect versus 3.5 mm non-critical size, pre-irradiated defect) may result in different VEGF release kinetics and implantation site environment, precluding a direct comparison of their results with this work.

Bone formation was also quantified at 12 weeks. The DUAL and BMP-2 groups showed similar amounts of bone formation, but both were significantly higher than the other groups. Because few studies have evaluated dual growth factor delivery for bone regeneration at an orthotopic site, comparison with previous work is limited. One study involved transplanted mesenchymal stem cells delivered with BMP-2 (4 μg) and TGF-β3 (0.4 μg) from alginate hydrogels in a mouse subcutaneous model [52]. There was significant ectopic bone formation when growth factors were delivered together when compared to individual delivery. A subsequent study by Oest et al. [53] examined the effects of these two growth factors *in vivo* in a critical size rat segmental defect, but using significantly smaller doses of the BMP-2 (0.2 μg) and TGF-β3 (0.02 μg) released from alginate within poly(L-lactide-*co*-D,L-lactide) scaffolds. Their results show only a small effect on bony bridging at 16 weeks, but do show similar results to this work in terms of higher bone formation (a strong trend at $p = 0.058$ was observed) from dual release groups over scaffold-only implants. However, no comparisons were made with single growth factor delivery of either BMP-2 or TGF-β3 alone.

The effect of single growth factor delivery of BMP-2 from poly(lactic-*co*-glycolic acid) scaffolds to a 5 mm rat cranial defect (not a critical size defect) has also been evaluated by microCT by Cowan et al. [39]. Varying doses of BMP-2 were used, ranging from 30–240 ng/mm^3. At 12 weeks, Cowan et al. noted ~60% bone volume for the 30 ng/mm^3 dose, but no bony bridging with this group. In contrast, we observed ~40% bone volume for a 40 ng/mm^3 dose (Figure 7) and bony bridging in an 8 mm critical size defect for 3 of the 8 animals in the BMP-2 group (Table 3).

In this study, the dual release group of VEGF and BMP-2 showed complete union of the defect in five out of eight of the rats, while BMP-2 showed union in only three out of the

eight rats (Table 3). Therefore, even though the quantity of bone was similar at 12 weeks, dual release resulted in more animals with union. This suggests again that the interplay between VEGF and BMP-2 for bone formation is beneficial, but also it is likely that the effects of dual release played out at some time between 4 and 12 weeks. Additionally, histological analysis showed that the quality of tissue response within the pores of the scaffold followed a similar trend – at 4 weeks, the DUAL group exhibited the highest scores against the others, but at 12 weeks, both DUAL and BMP-2 groups showed similar scores, and only the BMP-2 group was significantly better than its 4 week counterpart. Again, this suggests that the effect of dual release on bone formation occurs earlier than for BMP-2 alone. As described above, the work by Akita et al. showed significantly higher bone mineral density for dual release of BMP-2 and bFGF (with mesenchymal stem cells) at 4 weeks. However, at 8 weeks, there was no difference between the dual release group and controls (but again, no comparisons were made with single growth factor delivery), leading them to conclude that healing is accelerated by the dual delivery of the growth factors with the cells [45]. Similarly, the dual release of VEGF and BMP-2 in our system may have already resulted in faster bridging of the defect, for example at 8 or 10 weeks, and this effect is not seen at 12 weeks because BMP-2 release alone also results in bridging, but at a slower rate. Thus, an intermediate time point such as 8 weeks may be more appropriate for future studies investigating dual release constructs in this animal model.

This study sought to evaluate the effects of dual release of VEGF and BMP-2 from gelatin microparticles within porous PPF scaffolds on the healing of 8 mm critical size rat cranial defects. Although dual release had no effect on blood vessel formation at 4 weeks, bone formation was significantly higher than with other groups at that time period. At 12 weeks, dual release showed similar amounts of bone formation with BMP-2 groups, but a larger number of animals exhibited healing of the defect by bony bridging with dual release groups. Our results suggest that a synergistic effect can be seen at early time periods with dual release and may also result in faster healing times. Further investigations will focus on evaluating dose-dependent effects on both blood vessel and bone formation.

Acknowledgments

This work was supported by a grant from the National Institutes of Health (R01-DE15164) (AGM) and by a National Science Foundation Graduate Research Fellowship (ZSP). ZSP and SY would like to acknowledge the help of Ryan McGuire in preparing the specimens for histological sectioning.

Abbreviations

BLANK	implant group containing no growth factor within the scaffold
BMP-2	bone morphogenetic protein-2, and also implant group containing this growth factor within the scaffold
CSD	critical size defect
DUAL	implant group containing both VEGF and BMP-2 within the scaffold
EMPTY	group which had no scaffold implanted within the defect
microCT	microcomputed tomography
PBS	phosphate buffered saline
PPF	poly(propylene fumarate)
VEGF	vascular endothelial growth factor, and also implant group containing this growth factor within the scaffold

VOI volume of interest

References

1. Praemer, A.; Furner, S.; Rice, DP. Musculoskeletal Conditions in the United States. Rosemont: American Academy of Orthopaedic Surgeons; 1999.
2. Glowacki J. Angiogenesis in fracture repair. Clin Orthop 1998:S82–9. [PubMed: 9917629]
3. Carano RA, Filvaroff EH. Angiogenesis and bone repair. Drug Discov Today 2003;8:980–9. [PubMed: 14643161]
4. Gerber HP, Ferrara N. Angiogenesis and bone growth. Trends Cardiovasc Med 2000;10:223–8. [PubMed: 11282299]
5. Schmid J, Wallkamm B, Hammerle CH, Gogolewski S, Lang NP. The significance of angiogenesis in guided bone regeneration. A case report of a rabbit experiment. Clin Oral Implants Res 1997;8:244–8. [PubMed: 9586469]
6. Winet H. The role of microvasculature in normal and perturbed bone healing as revealed by intravital microscopy. Bone 1996;19:39S–57S. [PubMed: 8830997]
7. Winet H, Bao JY, Moffat R. A control model for tibial cortex neovascularization in the bone chamber. J Bone Miner Res 1990;5:19–30. [PubMed: 1689926]
8. Sojo K, Sawaki Y, Hattori H, Mizutani H, Ueda M. Immunohistochemical study of vascular endothelial growth factor (VEGF) and bone morphogenetic protein-2, -4 (BMP-2, -4) on lengthened rat femurs. J Craniomaxillofac Surg 2005;33:238–45. [PubMed: 15979317]
9. Street J, Bao M, deGuzman L, Bunting S, Peale FV Jr, Ferrara N, Steinmetz H, Hoeffel J, Cleland JL, Daugherty A, van Bruggen N, Redmond HP, Carano RA, Filvaroff EH. Vascular endothelial growth factor stimulates bone repair by promoting angiogenesis and bone turnover. Proc Natl Acad Sci U S A 2002;99:9656–61. [PubMed: 12118119]
10. Gerber HP, Vu TH, Ryan AM, Kowalski J, Werb Z, Ferrara N. VEGF couples hypertrophic cartilage remodeling, ossification and angiogenesis during endochondral bone formation. Nat Med 1999;5:623–8. [PubMed: 10371499]
11. Deckers MM, Karperien M, van der Bent C, Yamashita T, Papapoulos SE, Lowik CW. Expression of vascular endothelial growth factors and their receptors during osteoblast differentiation. Endocrinology 2000;141:1667–74. [PubMed: 10803575]
12. Pufe T, Wildemann B, Petersen W, Mentlein R, Raschke M, Schmidmaier G. Quantitative measurement of the splice variants 120 and 164 of the angiogenic peptide vascular endothelial growth factor in the time flow of fracture healing: a study in the rat. Cell Tissue Res 2002;309:387–92. [PubMed: 12195295]
13. Bostrom MP. Expression of bone morphogenetic proteins in fracture healing. Clin Orthop 1998:S116–23. [PubMed: 9917632]
14. Lutolf MP, Weber FE, Schmoekel HG, Schense JC, Kohler T, Muller R, Hubbell JA. Repair of bone defects using synthetic mimetics of collagenous extracellular matrices. Nat Biotechnol 2003;21:513–8. [PubMed: 12704396]
15. Chang SC, Chuang H, Chen YR, Yang LC, Chen JK, Mardinis S, Chung HY, Lu YL, Ma WC, Lou J. Cranial repair using BMP-2 gene engineered bone marrow stromal cells. J Surg Res 2004;119:85–91. [PubMed: 15126087]
16. Duggirala SS, Rodgers JB, DeLuca PP. The evaluation of lyophilized polymer matrices for administering recombinant human bone morphogenetic protein-2. Pharm Dev Technol 1996;1:165–74. [PubMed: 9552343]
17. Puleo DA, Huh WW, Duggirala SS, DeLuca PP. In vitro cellular responses to bioerodible particles loaded with recombinant human bone morphogenetic protein-2. J Biomed Mater Res 1998;41:104–10. [PubMed: 9641630]
18. Murakami N, Saito N, Takahashi J, Ota H, Horiuchi H, Nawata M, Okada T, Nozaki K, Takaoka K. Repair of a proximal femoral bone defect in dogs using a porous surfaced prosthesis in combination with recombinant BMP-2 and a synthetic polymer carrier. Biomaterials 2003;24:2153–9. [PubMed: 12699651]

19. Kakudo N, Kusumoto K, Wang YB, Iguchi Y, Ogawa Y. Immunolocalization of vascular endothelial growth factor on intramuscular ectopic osteoinduction by bone morphogenetic protein-2. Life Sci 2006;79:1847–55. Epub 2006 Jun 27. [PubMed: 16857215]
20. Patel ZS, Ueda H, Yamamoto M, Tabata Y, Mikos AG. In vitro and in vivo release of vascular endothelial growth factor from gelatin microparticles and biodegradable composite scaffolds. Pharmaceutical Research. 2008 (in press).
21. Patel ZS, Yamamoto M, Ueda H, Tabata Y, Mikos AG. Biodegradable gelatin microparticles as delivery systems for the controlled release of bone morphogenetic protein-2. Acta Biomaterialia. 2008 (in press).
22. Hedberg EL, Kroese-Deutman HC, Shih CK, Crowther RS, Carney DH, Mikos AG, Jansen JA. In vivo degradation of porous poly(propylene fumarate)/poly(DL-lactic-co-glycolic acid) composite scaffolds. Biomaterials 2005;26:4616–23. Epub 2005 Jan 18. [PubMed: 15722131]
23. Fisher JP, Vehof JW, Dean D, van der Waerden JP, Holland TA, Mikos AG, Jansen JA. Soft and hard tissue response to photocrosslinked poly(propylene fumarate) scaffolds in a rabbit model. J Biomed Mater Res 2002;59:547–56. [PubMed: 11774313]
24. Guldberg RE, Ballock RT, Boyan BD, Duvall CL, Lin AS, Nagaraja S, Oest M, Phillips J, Porter BD, Robertson G, Taylor WR. Analyzing bone, blood vessels, and biomaterials with microcomputed tomography. IEEE Eng Med Biol Mag 2003;22:77–83. [PubMed: 14699940]
25. Lee KY, Peters MC, Mooney DJ. Comparison of vascular endothelial growth factor and basic fibroblast growth factor on angiogenesis in SCID mice. J Control Release 2003;87:49–56. [PubMed: 12618022]
26. Yamamoto M, Takahashi Y, Tabata Y. Controlled release by biodegradable hydrogels enhances the ectopic bone formation of bone morphogenetic protein. Biomaterials 2003;24:4375–83. [PubMed: 12922150]
27. Blum JS, Barry MA, Mikos AG, Jansen JA. In vivo evaluation of gene therapy vectors in ex vivo-derived marrow stromal cells for bone regeneration in a rat critical-size calvarial defect model. Hum Gene Ther 2003;14:1689–701. [PubMed: 14670121]
28. Castano-Izquierdo H, Alvarez-Barreto J, van den Dolder J, Jansen JA, Mikos AG, Sikavitsas VI. Pre-culture period of mesenchymal stem cells in osteogenic media influences their in vivo bone forming potential. J Biomed Mater Res A 2007;82:129–38. [PubMed: 17269144]
29. Kasper FK, Young S, Tanahashi K, Barry MA, Tabata Y, Jansen JA, Mikos AG. Evaluation of bone regeneration by DNA release from composites of oligo(poly(ethylene glycol) fumarate) and cationized gelatin microspheres in a critical-sized calvarial defect. J Biomed Mater Res A 2006;78:335–42. [PubMed: 16639744]
30. Sikavitsas VI, van den Dolder J, Bancroft GN, Jansen JA, Mikos AG. Influence of the in vitro culture period on the in vivo performance of cell/titanium bone tissue-engineered constructs using a rat cranial critical size defect model. J Biomed Mater Res A 2003;67:944–51. [PubMed: 14613243]
31. Bodde EW, Boerman OC, Russel FG, Mikos AG, Spauwen PH, Jansen JA. The kinetic and biological activity of different loaded rhBMP-2 calcium phosphate cement implants in rats. J Biomed Mater Res A 2008;15:15.
32. Ruhe PQ, Hedberg EL, Padron NT, Spauwen PH, Jansen JA, Mikos AG. Biocompatibility and degradation of poly(DL-lactic-co-glycolic acid)/calcium phosphate cement composites. J Biomed Mater Res A 2005;74:533–44. [PubMed: 16041795]
33. Ruhe PQ, Hedberg-Dirk EL, Padron NT, Spauwen PH, Jansen JA, Mikos AG. Porous poly(DL-lactic-co-glycolic acid)/calcium phosphate cement composite for reconstruction of bone defects. Tissue Eng 2006;12:789–800. [PubMed: 16674292]
34. Holland TA, Tabata Y, Mikos AG. *In vitro* release of transforming growth factor-beta1 from gelatin microparticles encapsulated in biodegradable, injectable oligo(poly(ethylene glycol) fumarate) hydrogels. J Control Release 2003;91:299–313. [PubMed: 12932709]
35. Shung AK, Behravesh E, Jo S, Mikos AG. Crosslinking characteristics of and cell adhesion to an injectable poly(propylene fumarate-co-ethylene glycol) hydrogel using a water-soluble crosslinking system. Tissue Eng 2003;9:243–54. [PubMed: 12740087]

36. Porter BD, Oldham JB, He SL, Zobitz ME, Payne RG, An KN, Currier BL, Mikos AG, Yaszemski MJ. Mechanical properties of a biodegradable bone regeneration scaffold. J Biomech Eng 2000;122:286–8. [PubMed: 10923298]
37. Hedberg EL, Kroese-Deutman HC, Shih CK, Crowther RS, Carney DH, Mikos AG, Jansen JA. Effect of varied release kinetics of the osteogenic thrombin peptide TP508 from biodegradable, polymeric scaffolds on bone formation in vivo. J Biomed Mater Res A 2005;72:343–53. [PubMed: 15666357]
38. van der Lubbe HB, Klein CP, de Groot K. A simple method for preparing thin (10 microM) histological sections of undecalcified plastic embedded bone with implants. Stain Technol 1988;63:171–6. [PubMed: 2459815]
39. Cowan CM, Aghaloo T, Chou YF, Walder B, Zhang X, Soo C, Ting K, Wu B. MicroCT evaluation of three-dimensional mineralization in response to BMP-2 doses in vitro and in critical sized rat calvarial defects. Tissue Eng 2007;13:501–12. [PubMed: 17319794]
40. Duvall CL, Robert Taylor W, Weiss D, Guldberg RE. Quantitative microcomputed tomography analysis of collateral vessel development after ischemic injury. Am J Physiol Heart Circ Physiol 2004;287:H302–10. [PubMed: 15016633]
41. Murphy WL, Simmons CA, Kaigler D, Mooney DJ. Bone regeneration via a mineral substrate and induced angiogenesis. J Dent Res 2004;83:204–10. [PubMed: 14981120]
42. Leach JK, Kaigler D, Wang Z, Krebsbach PH, Mooney DJ. Coating of VEGF-releasing scaffolds with bioactive glass for angiogenesis and bone regeneration. Biomaterials 2006;27:3249–55. Epub 2006 Feb 21. [PubMed: 16490250]
43. Richardson TP, Peters MC, Ennett AB, Mooney DJ. Polymeric system for dual growth factor delivery. Nat Biotechnol 2001;19:1029–1034. [PubMed: 11689847]
44. Rai B, Oest ME, Dupont KM, Ho KH, Teoh SH, Guldberg RE. Combination of platelet-rich plasma with polycaprolactone-tricalcium phosphate scaffolds for segmental bone defect repair. J Biomed Mater Res A 2007;81:888–99. [PubMed: 17236215]
45. Akita S, Fukui M, Nakagawa H, Fujii T, Akino K. Cranial bone defect healing is accelerated by mesenchymal stem cells induced by coadministration of bone morphogenetic protein-2 and basic fibroblast growth factor. Wound Repair Regen 2004;12:252–9. [PubMed: 15086777]
46. Mayr-Wohlfart U, Waltenberger J, Hausser H, Kessler S, Gunther KP, Dehio C, Puhl W, Brenner RE. Vascular endothelial growth factor stimulates chemotactic migration of primary human osteoblasts. Bone 2002;30:472–7. [PubMed: 11882460]
47. Midy V, Plouet J. Vasculotropin/vascular endothelial growth factor induces differentiation in cultured osteoblasts. Biochem Biophys Res Commun 1994;199:380–6. [PubMed: 8123039]
48. Deckers MM, van Bezooijen RL, van der Horst G, Hoogendam J, van Der Bent C, Papapoulos SE, Lowik CW. Bone morphogenetic proteins stimulate angiogenesis through osteoblast-derived vascular endothelial growth factor A. Endocrinology 2002;143:1545–53. [PubMed: 11897714]
49. Raida M, Heymann AC, Gunther C, Niederwieser D. Role of bone morphogenetic protein 2 in the crosstalk between endothelial progenitor cells and mesenchymal stem cells. Int J Mol Med 2006;18:735–9. [PubMed: 16964430]
50. Kaigler D, Wang Z, Horger K, Mooney DJ, Krebsbach PH. VEGF scaffolds enhance angiogenesis and bone regeneration in irradiated osseous defects. J Bone Miner Res 2006;21:735–44. [PubMed: 16734388]
51. Leach JB, Bivens KA, Patrick CW Jr, Schmidt CE. Photocrosslinked hyaluronic acid hydrogels: Natural, biodegradable tissue engineering scaffolds. Biotech Bioeng 2003;82:578–589.
52. Simmons CA, Alsberg E, Hsiong S, Kim WJ, Mooney DJ. Dual growth factor delivery and controlled scaffold degradation enhance in vivo bone formation by transplanted bone marrow stromal cells. Bone 2004;35:562–9. [PubMed: 15268909]
53. Oest ME, Dupont KM, Kong HJ, Mooney DJ, Guldberg RE. Quantitative assessment of scaffold and growth factor-mediated repair of critically sized bone defects. J Orthop Res 2007;25:941–50. [PubMed: 17415756]

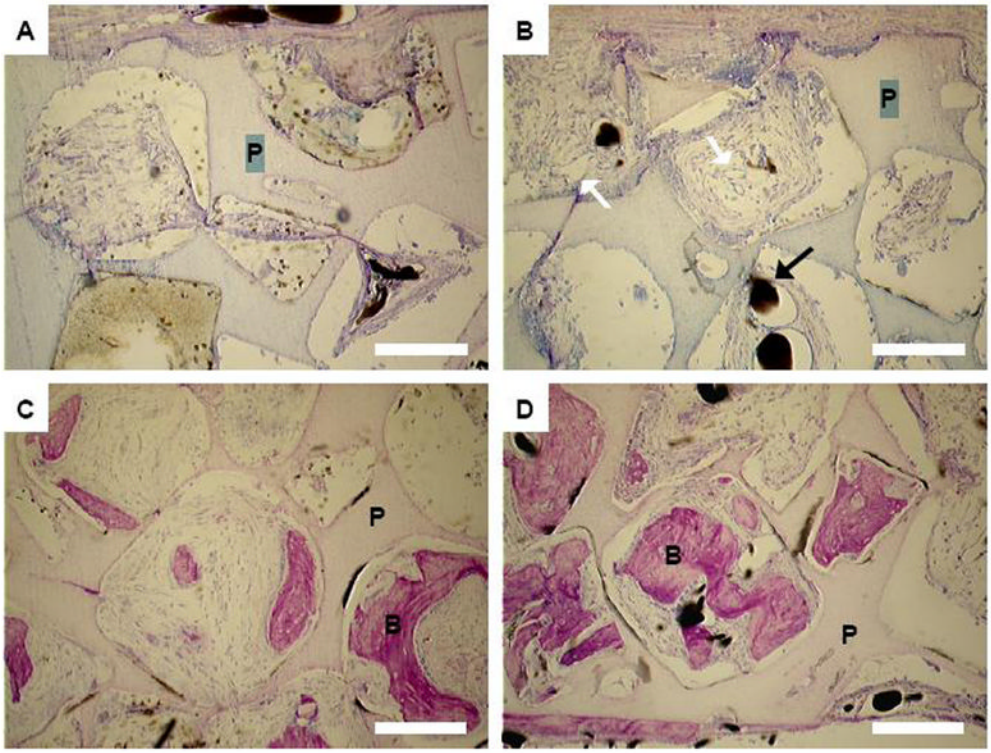

Figure 1. Histological sections of composite scaffolds at 4 weeks

Fibrous tissue infiltration was observed in A) BLANK and B) VEGF groups, while some bone formation was observed in C) BMP-2 and D) DUAL groups. In B), the black arrow points to Microfil within a blood vessel, while the white arrows point to unperfused blood vessels. **P:** PPF scaffold; **B:** new bone. Bar represents 200 μm for all panels.

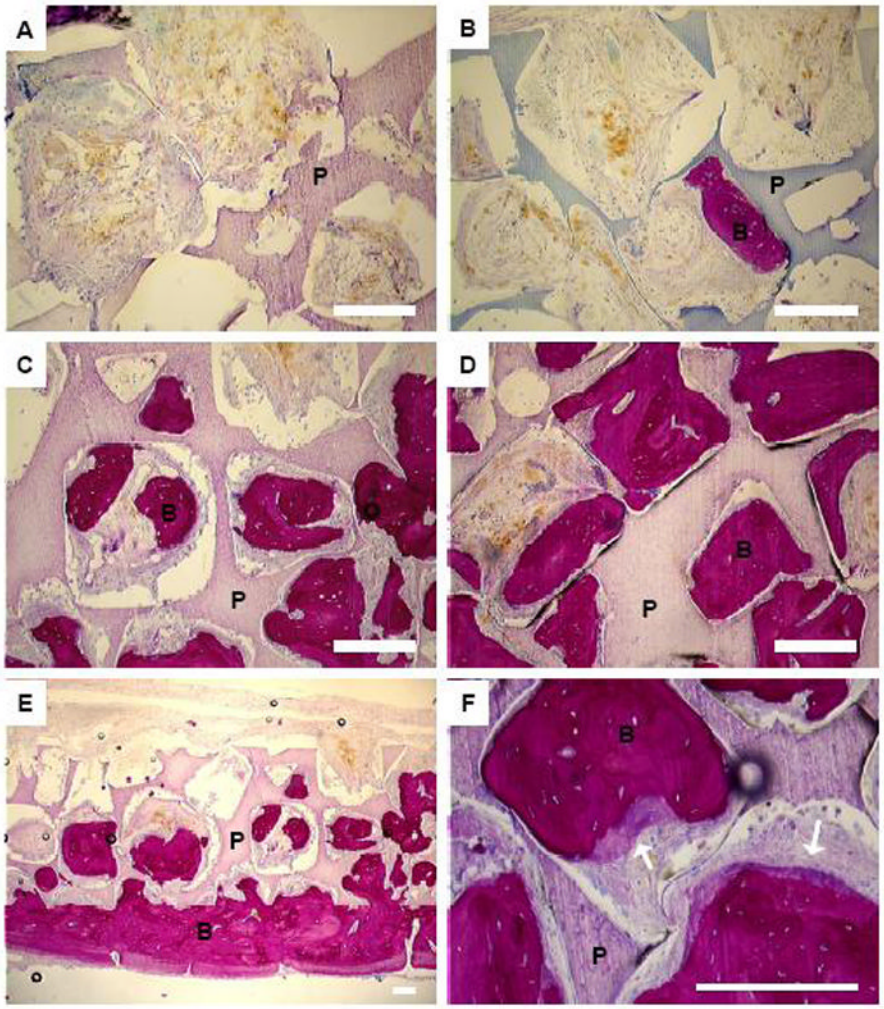

Figure 2. Histological sections of composite scaffolds at 12 weeks

In the A) BLANK and B) VEGF groups, the ingrowth tissue was mostly fibrous with minimal bone formation. However, in the C) BMP-2 and D) DUAL groups, there was significant bone formation in both the pores and along the scaffold surfaces, generally observed on the dural side (panel E, BMP-2 group). Intramembranous ossification (panel F, BMP-2 group) was characterized by osteoid secretion and mineralization (white arrows). **P:** PPF scaffold; **B:** new bone. Bar represents 200 μm for all panels.

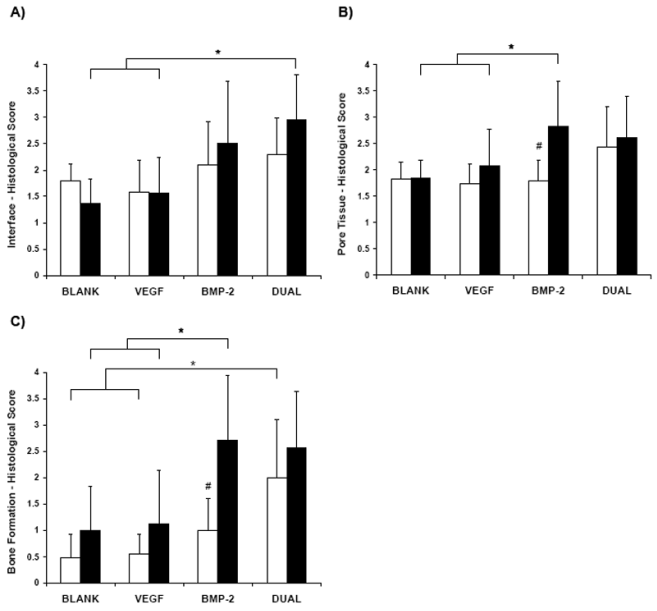

Figure 3. Results of histological scoring

Scores for A) the hard tissue response at the bone-scaffold interface, B) the tissue response within the scaffold pores, and C) the amount of bone formation within the defect at 4 weeks (□) and 12 weeks (■) for the four groups examined in this study (BLANK, VEGF, BMP-2, and DUAL). Error bars represent standard deviation for $n = 8–9$. (*) denotes statistical significance at $p<0.05$. (#) denotes statistical significance at $p<0.05$ compared to the BMP-2 group at 12 weeks.

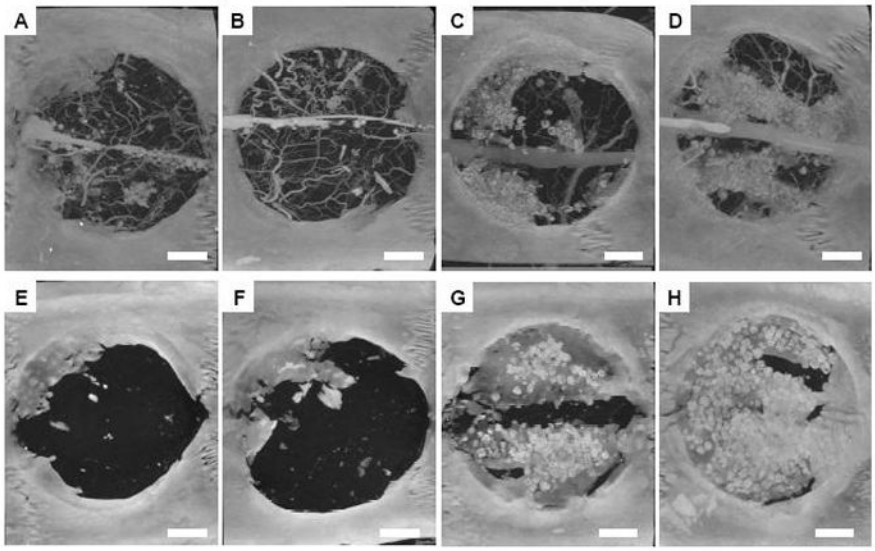

Figure 4. MicroCT images (maximum intensity projections) of cranial defects at 4 and 12 weeks
Panels A–D represent BLANK, VEGF, BMP-2, and DUAL groups at 4 weeks prior to decalcification; both blood vessels and bone were visible. Panels E–H represent BLANK, VEGF, BMP-2, and DUAL groups at 12 weeks; no blood vessels were visible because Microfil perfusion was not done at this time period. Bar represents 200 μm for all panels.

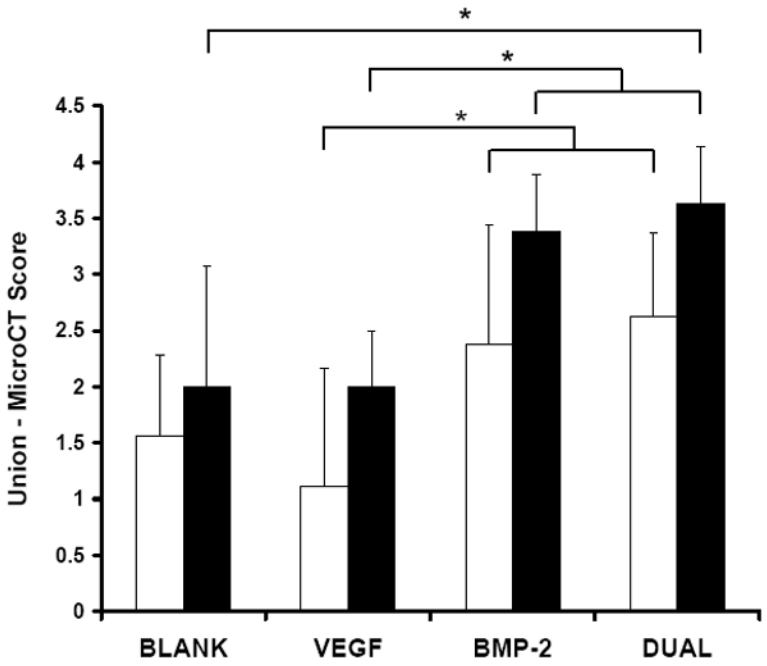

Figure 5. Results of scoring for bony bridging and union within the defect

Scores for bony bridging and union for the four groups (BLANK, VEGF, BMP-2, and DUAL) examined at 4 weeks (□) and 12 weeks (■). Error bars represent standard deviation for n = 8–9. (*) denotes statistical significance ($p<0.05$) between groups.

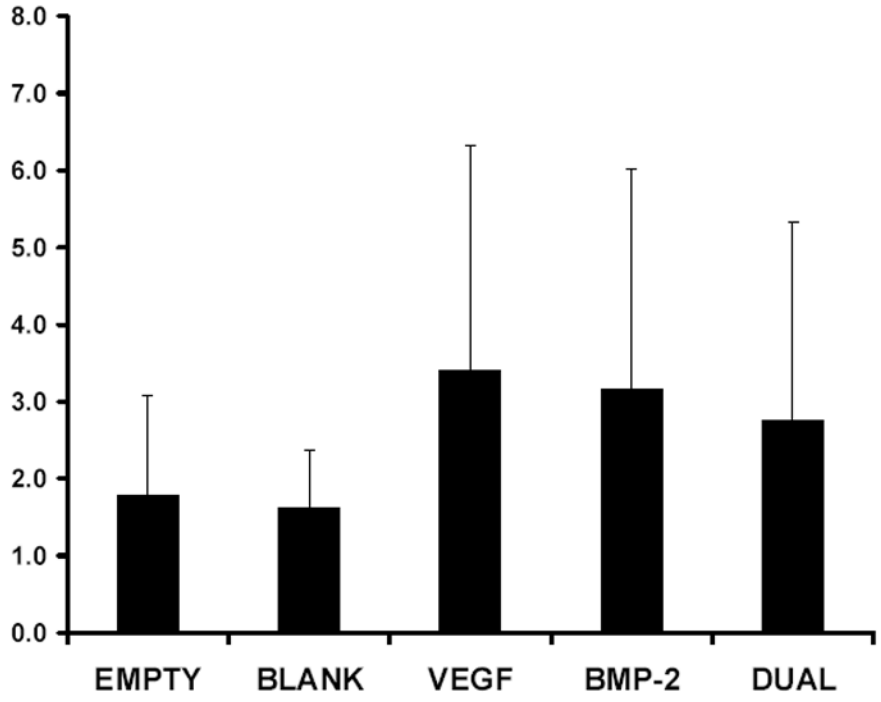

Figure 6. Results of microCT quantification of % blood vessel volume within the defect at 4 weeks

Values for % blood vessel volume are given for the four groups (BLANK, VEGF, BMP-2, and DUAL) examined as well as the EMPTY group as quantified by microCT. Error bars represent standard deviation for $n = 8–9$.

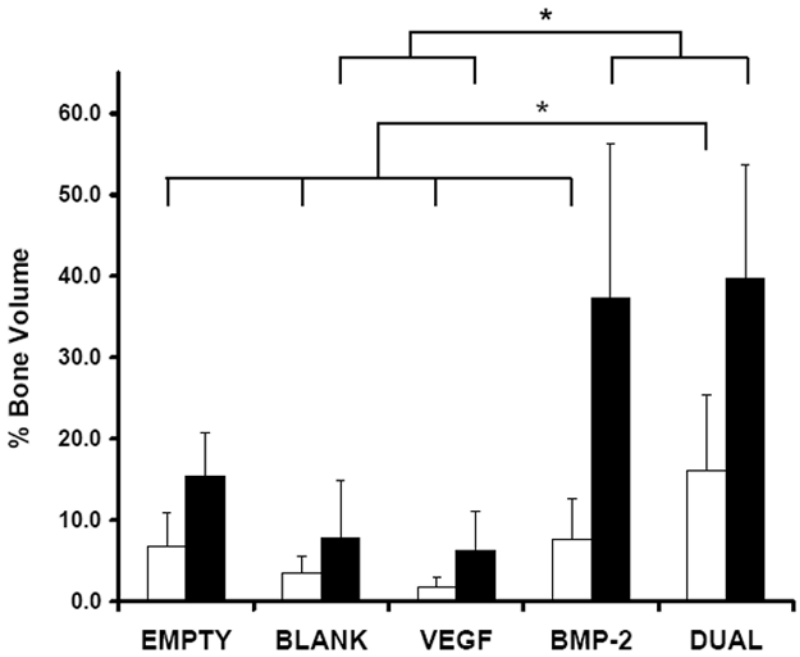

Figure 7. Results of microCT quantification of % bone volume within the defect at 4 and 12 weeks

Values are given for % bone volume of the four groups (BLANK, VEGF, BMP-2, and DUAL) examined as well as the EMPTY group as quantified by microCT. Error bars represent standard deviation for $n = 8–9$. At 4 weeks (□), the DUAL group was significantly different ($p<0.05$) than all other groups. At 12 weeks (■), both DUAL and BMP-2 groups were significantly different ($p<0.05$) from VEGF and BLANK groups.

Table 1

Scoring guide for extent of bony bridging and union using microCT datasets.

Description	Score
Bony bridging entire span of defect at longest point (8 mm)	4
Bony bridging over partial length of defect	3
Bony bridging only at defect borders	2
Few bony spicules dispersed through defect	1
No bone formation within defect	0

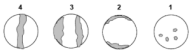

Table 2

Guide for quantitative histological analysis.

Hard tissue response at bone-scaffold Interface	
Description	**Score**
Direct bone to implant contact without soft tissue interlayer	4
Remodeling lacuna with osteoblasts and/or osteoclasts at surface	3
Majority of implant is surrounded by fibrous tissue capsule	2
Unorganized fibrous tissue (majority of tissue is not arranged as a capsule)	1
Inflammation marked by an abundance of inflammatory cells and poorly organized tissue	0
Hard tissue response within the pores of the scaffold	
Description	**Score**
Tissue in pores is mostly bone	4
Tissue in pores consists of some bone with mature, dense fibrous tissue and/or a few inflammatory response elements	3
Tissue in pores is mostly immature fibrous tissue (with or without bone) with blood vessels and young fibroblasts invading the space with few macrophages present	2
Tissue in pores consists mostly of inflammatory cells and connective tissue components in between (with or without bone) OR the majority of the pores are empty or filled with fluid	1
Tissue in pores is dense and exclusively of inflammatory type (no bone present)	0
Extent of bone formation within the defect	
Description	**Score**
75–100% of defect consists of bone	4
50–74% of defect consists of bone	3
25–49% of defect consists of bone	2
1–24% of defect consists of bone	1

Table 3

Quantitative results of 12 week samples for scoring of union.

Group	Scores	Samples with Total Union
BLANK	0,1,2,2,2,3,3,3	0/8
VEGF	1,2,2,2,2,2,2,3	0/9
BMP-2	3,3,3,3,3,4,4,4	3/8
DUAL	3,3,3,4,4,4,4,4	5/8